Molecular mechanisms regulating spines

1. F-actin, consisting of β- and γ-actin, is highly concentrated in spines whereas microtubules are generally sparse or missing.

2. The shape and stability of spine head and neck are determined largely by the actin cytoskeleton.

3. Proteins that bind to and modify the actin cytoskeleton are prime candidates for regulators of spine morphogenesis.

4. A-actinin, drebrin, spinophilin/neurabin II, adducin, RapGAP, and cortactin are specifically enriched in the spines.

5. Rho GTPases, Rho/Rac/Cdc42

Table 2 | **Molecular pathways that affect dendritic spines**

Protein/pathway	Biochemical function	Effect on spines	References
Rac, Kalirin-7 (a RacGEF)	Rac is a small GTPase that regulates the actin cytoskeleton through several effectors, including Pak kinase; RacGEFs activate Rac through GTP/GDP exchange	Active (GTP-bound) Rac increases the density of filopodia- and lamellipodia-like protrusions	70–73
RhoA	RhoA is a small GTPase that regulates the actin cytoskeleton through Rho kinase/ROCK	Activated RhoA leads to loss of spines in a subset of neurons	72
Ras/MAP kinase pathway	Ras is a small GTPase activated by receptor tyrosine kinases and stimulates the MAP kinase pathway	Activated Ras/MAP kinase is required for depolarization-induced filopodia formation	74
Rap, SPAR (a RapGAP)	Rap is a small GTPase closely related to Ras, but its targets are poorly understood. SPAR interacts with and reorganizes F-actin; as a RapGAP, SPAR also inhibits Rap activity	SPAR induces larger, more elaborate spine heads (dependent on its ability to bind PSD95 and reorganize F-actin); active Rap has been suggested to promote spine elongation	67
PSD95	PSD95 is an abundant scaffold protein of the PSD density that binds directly to NMDA receptors through its PDZ domains	Overexpression of PSD95 leads to increased number and size of spines, an effect that depends on the PDZ domains of PSD95, and correlates with recruitment of AMPA receptors	81
Shank	Shank is a multidomain scaffold protein in the PSD that binds to NMDA receptors and mGluR protein complexes	Shank causes enlargement of spine heads with no change in spine number, an effect that depends on the PDZ domain of Shank, and its ability to bind Homer	83
Syndecan 2	Syndecan 2 is a cell-surface heparan-sulphate proteoglycan with a cytoplasmic carboxyl terminus that binds PDZ proteins, such as CASK and synbindin	Syndecan 2 accelerates the maturation of spines, an effect that depends on PDZ-binding the carboxyl terminus of syndecan 2	77

AMPA, α-amino-3-hydroxy-5-methyl-4-isoxazole propionic acid; CASK, calcium/calmodulin-dependent serine protein kinase; F-actin, filamentous actin; GAP, GTPase-activating protein; MAP kinase, mitogen-activated protein kinase; mGluR, metabotropic glutamate receptor; NMDA, *N*-methyl-D-asparate; Pak, p21-activated kinase; PSD, postsynaptic density; GEF, guanine nucleotide exchange factor; ROCK, Rho-associated, coiled-coil-containing protein kinase; SPAR, spine-associated RapGAP.

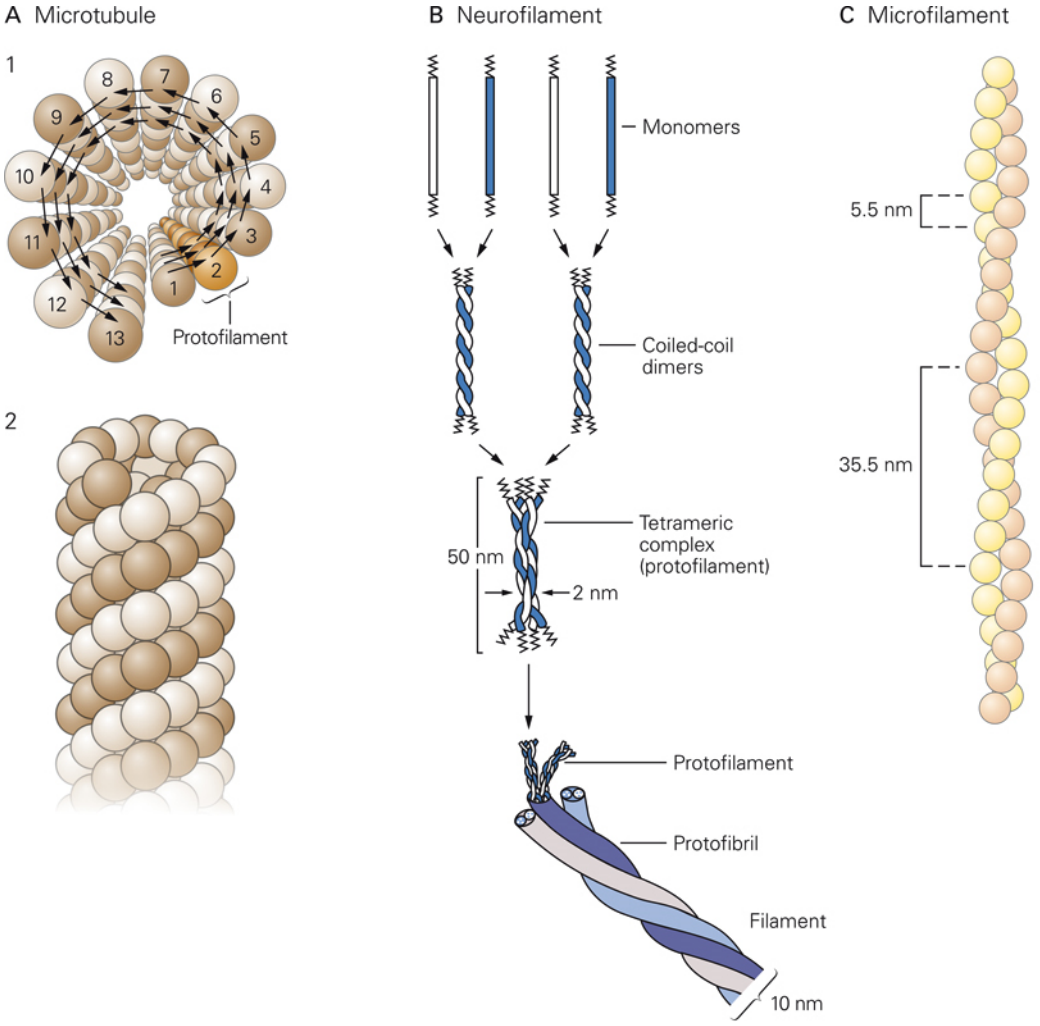

Figure 4–5 Atlas of fibrillary structures.

A. Microtubules, the largest-diameter fibers (25 nm), are helical cylinders composed of 13 protofilaments, each 5 nm in width. Each protofilament is made up of a column of alternating α- and β-tubulin subunits (each subunit has a molecular weight of approximately 50,000). Adjacent subunits bind to each along the longitudinal protofilaments and laterally between subunits of adjacent protofilaments.

A tubulin molecule is a heterodimer consisting of one α- and one β-tubulin subunit. **1.** View of a microtubule. The arrows indicate the direction of the right-handed helix. **2.** A side-view of a microtubule shows the alternating α- and β-subunits.

B. Neurofilaments are built with fibers that twist around each other to produce coils of increasing thickness. The thinnest units are monomers that form coiled-coil heterodimers. These dimers form a tetrameric complex that becomes the protofilament. Two protofilaments become a protofibril, and three protofibrils are helically twisted to form the 10 nm diameter neurofilament. (Adapted, with permission, from Bershadsky and Vasiliev 1988.)

C. Microfilaments, the smallest diameter fibers (approximately 7 nm), are composed of two strands of polymerized globular actin (G-actin) monomers arranged in a helix. At least six different (but closely related) actins are found in mammals. Each variant is encoded by a separate gene. Microfilaments are polar structures because the globular monomers are asymmetric.

Highly phosphorylted tau

β-amyloid peptides

α-synuclein etc.

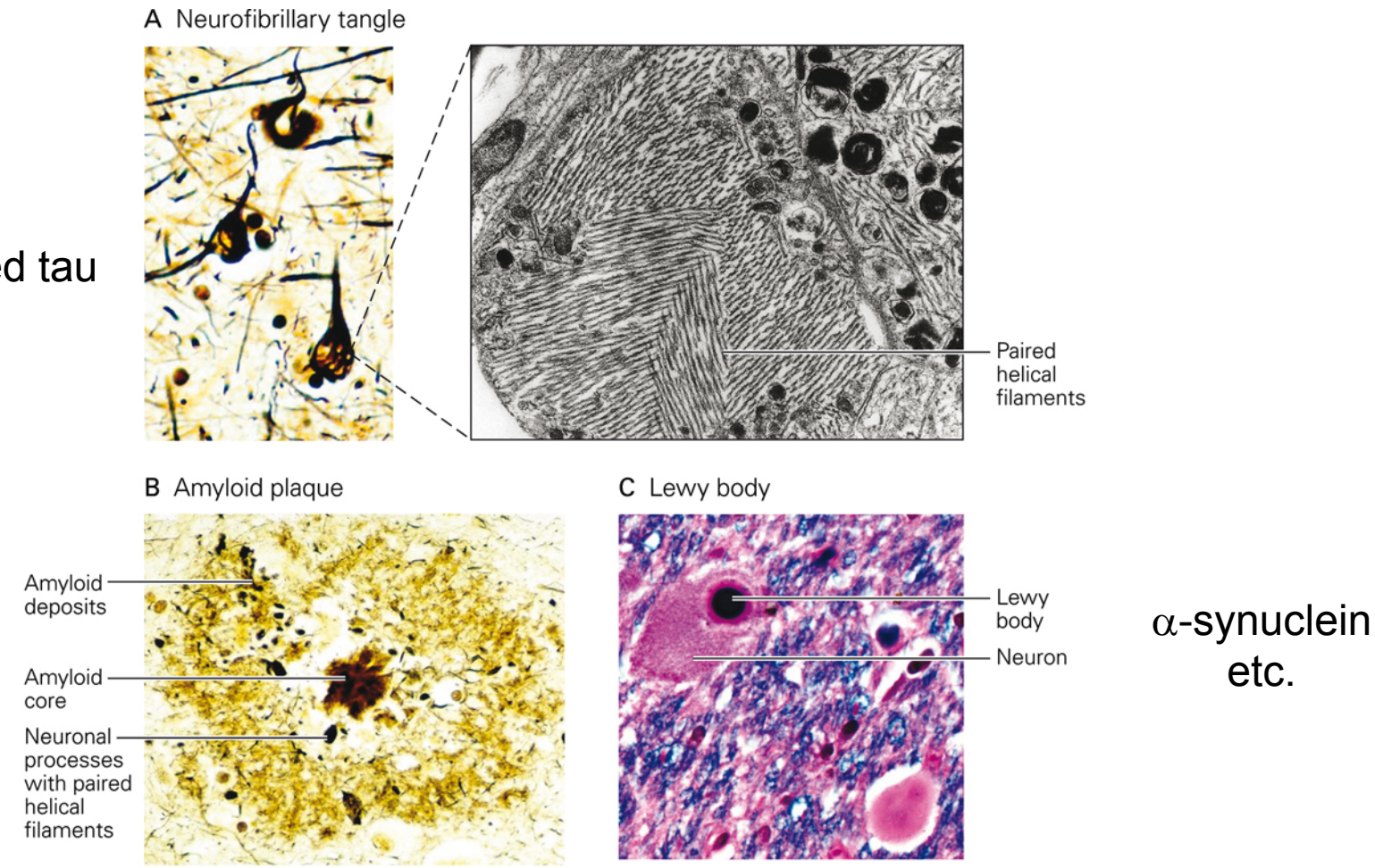

Figure 4–6 Abnormal aggregates of proteins inside neurons in Alzheimer and Parkinson diseases.

A. Intracellular neurofibrillary tangles of Alzheimer disease, labeled here with a dark silver stain (left). (Reproduced, with permission, from J.P. Vonsattel.) The electron micrograph of a tangle (right) shows the bundles of abnormal filaments, here filling a dendrite. The filaments are composed of altered tau protein. (Reproduced, with permission, from Esiri et al. 2002.)

B. Extracellular deposits of polymerized β-amyloid peptides in Alzheimer disease create an amyloid plaque. This plaque has a dense core of amyloid as well as a surrounding halo of deposits. Note the neuronal processes in the plaque with tangle pathology. (Reproduced, with permission, from J.P. Vonsattel.)

C. A Lewy body in the substantia nigra of a patient with Parkinson disease contains accumulations of abnormal filaments made up of α-synuclein, among other proteins. (Reproduced, with permission, from J.P. Vonsattel.)

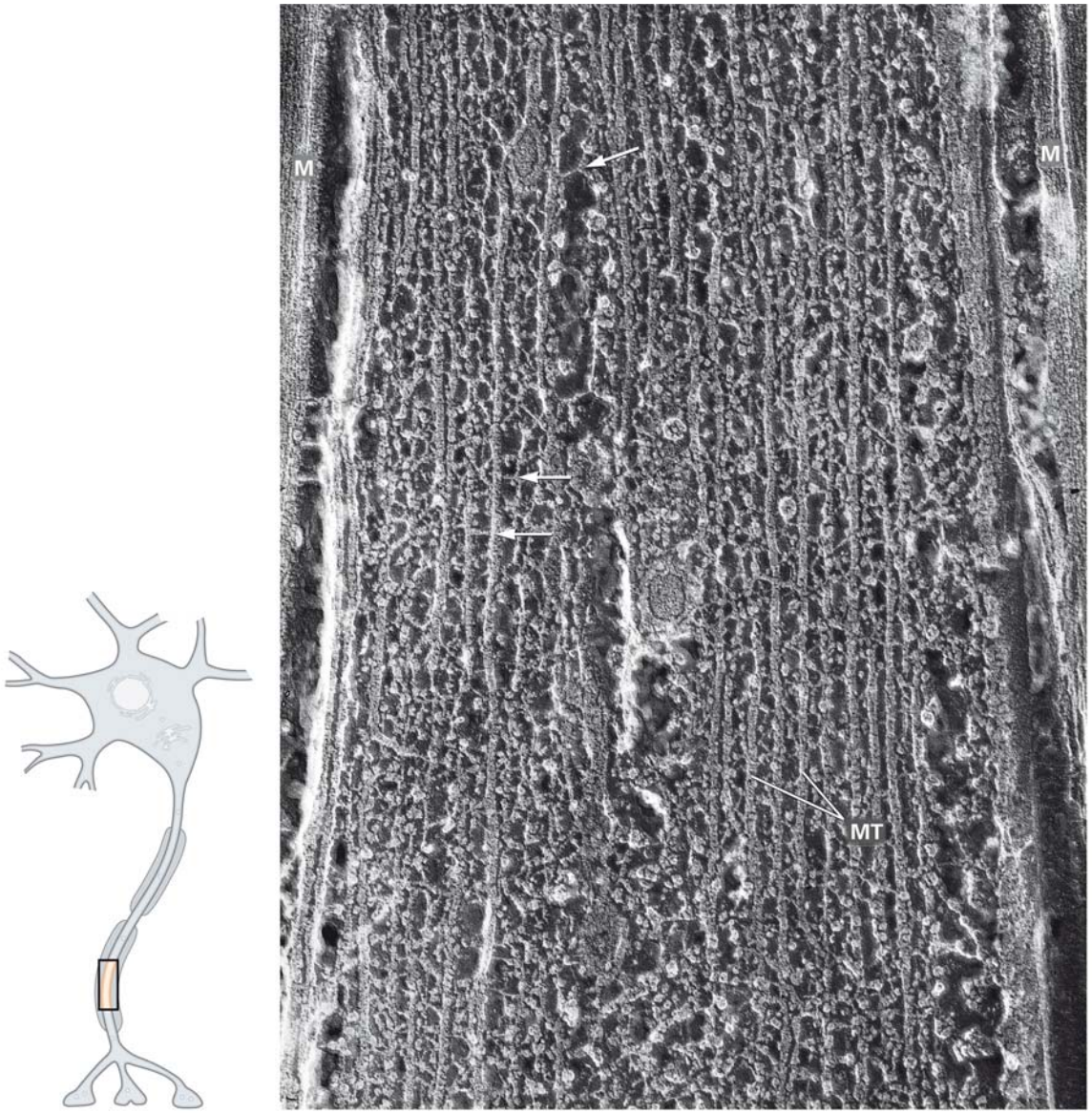

Figure 4–7 The cytoskeletal structure of an axon. The micrograph shows the dense packing of microtubules and neurofilaments linked by cross bridges (**arrows**). Organelles are transported in both the anterograde and retrograde directions in the microtubule-rich domains. Visualization in the micrograph was achieved by quick freezing and deep etching. **M,** myelin sheath; **MT**, microtubules × 105,000. (Adapted, with permission, from Schnapp and Reese 1982.)

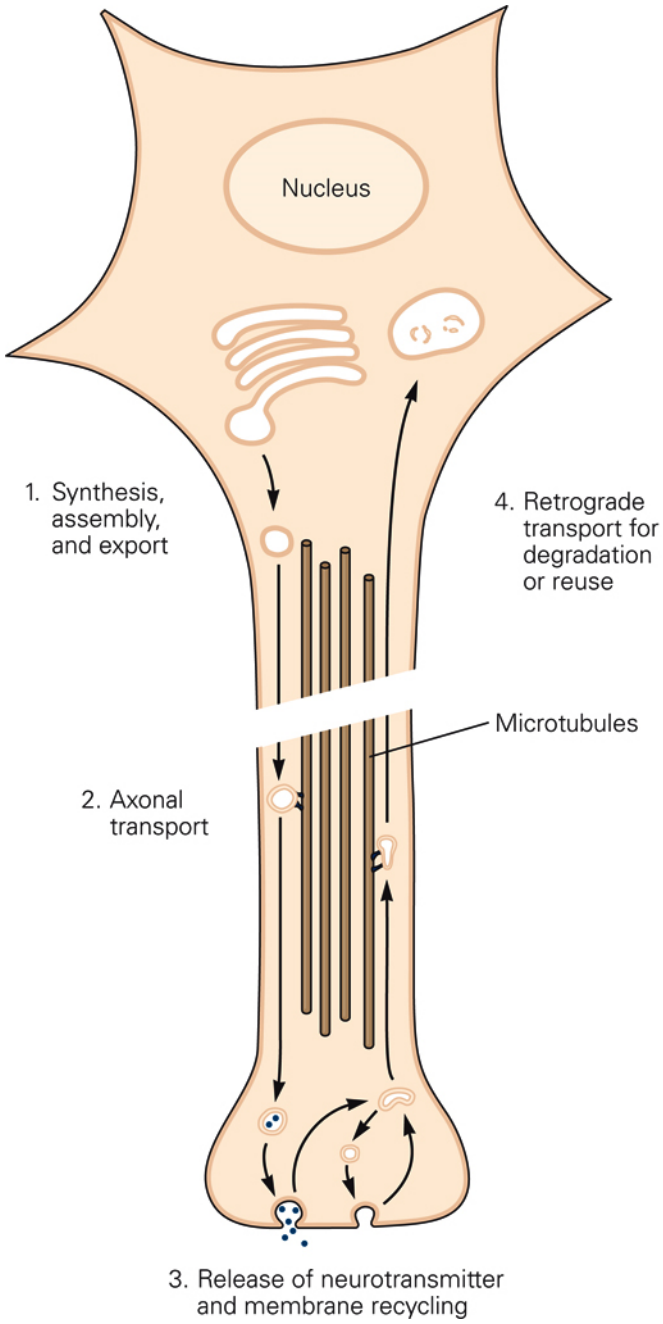

Fast axonal transport: 200-400 mm/day
(2-5 μm/s)
Slow axonal transport: 0.17-8.6 mm/day
(0.002-0.1 μm/s)

Anterograde transport
Retrograde transport

Figure 4–8 **Membrane trafficking in the neuron. 1.** Proteins and lipids of secretory organelles are synthesized in the endoplasmic reticulum and transported to the Golgi complex, where large dense-core vesicles (peptide-containing secretory granules) and synaptic vesicle precursors are assembled. **2.** Large dense-core vesicles and transport vesicles that carry synaptic vesicle proteins travel down the axon via axonal transport. **3.** At the nerve terminals the synaptic vesicles are assembled and loaded with nonpeptide neurotransmitters. Synaptic vesicles and large dense-core vesicles release their contents by exocytosis. **4.** Following exocytosis, large dense-core vesicle membranes are returned to the cell body for reuse or degradation. Synaptic vesicle membranes undergo many cycles of local exocytosis and endocytosis in the presynaptic terminal.

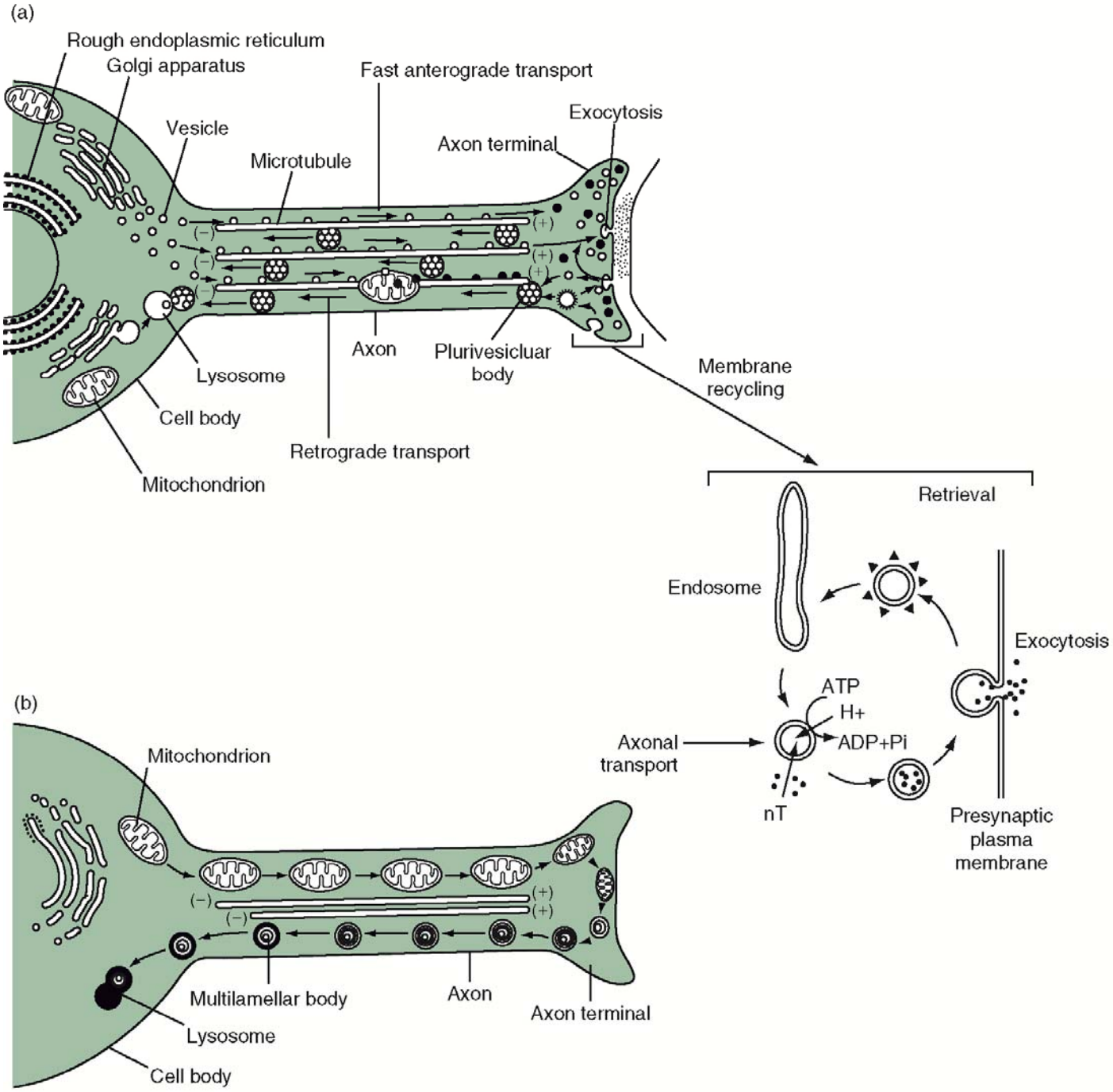

FIGURE 1.10 Fast axonal transport.

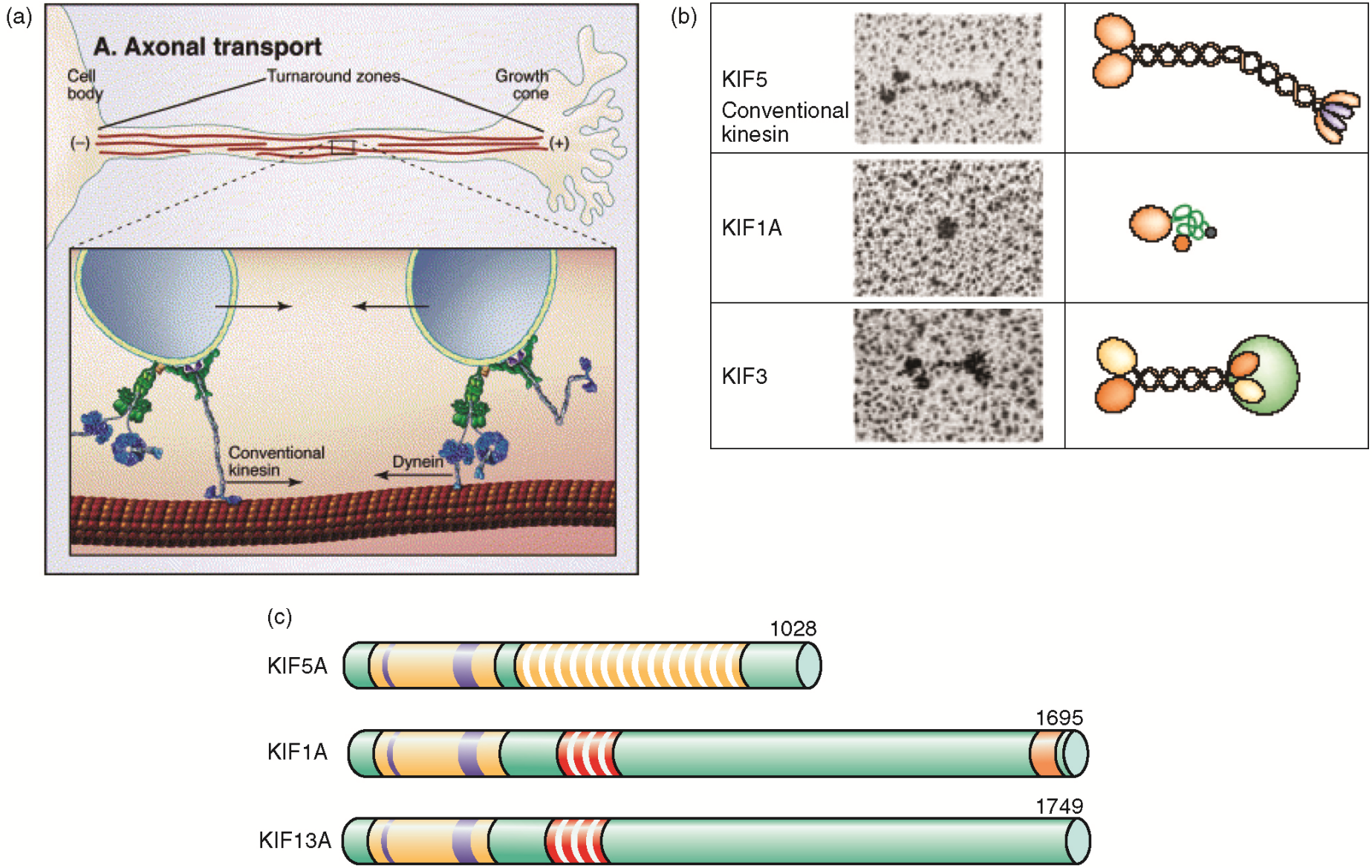

FIGURE 1.11 The motors of fast anterograde and retrograde axonal transport.

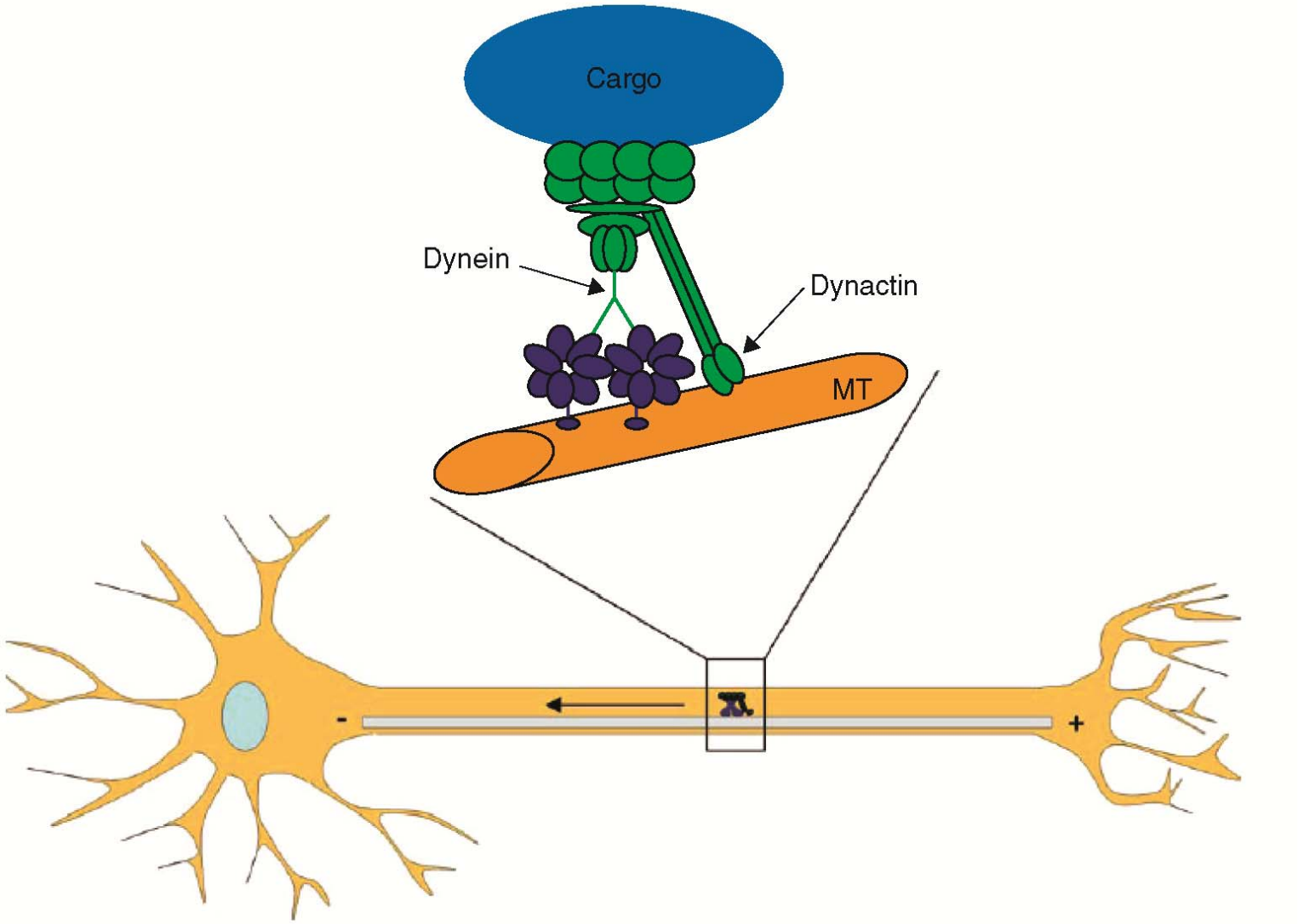

FIGURE 1.12 Cytoplasmic dynein and dynactin drive retrograde axonal transport in motor neurons.

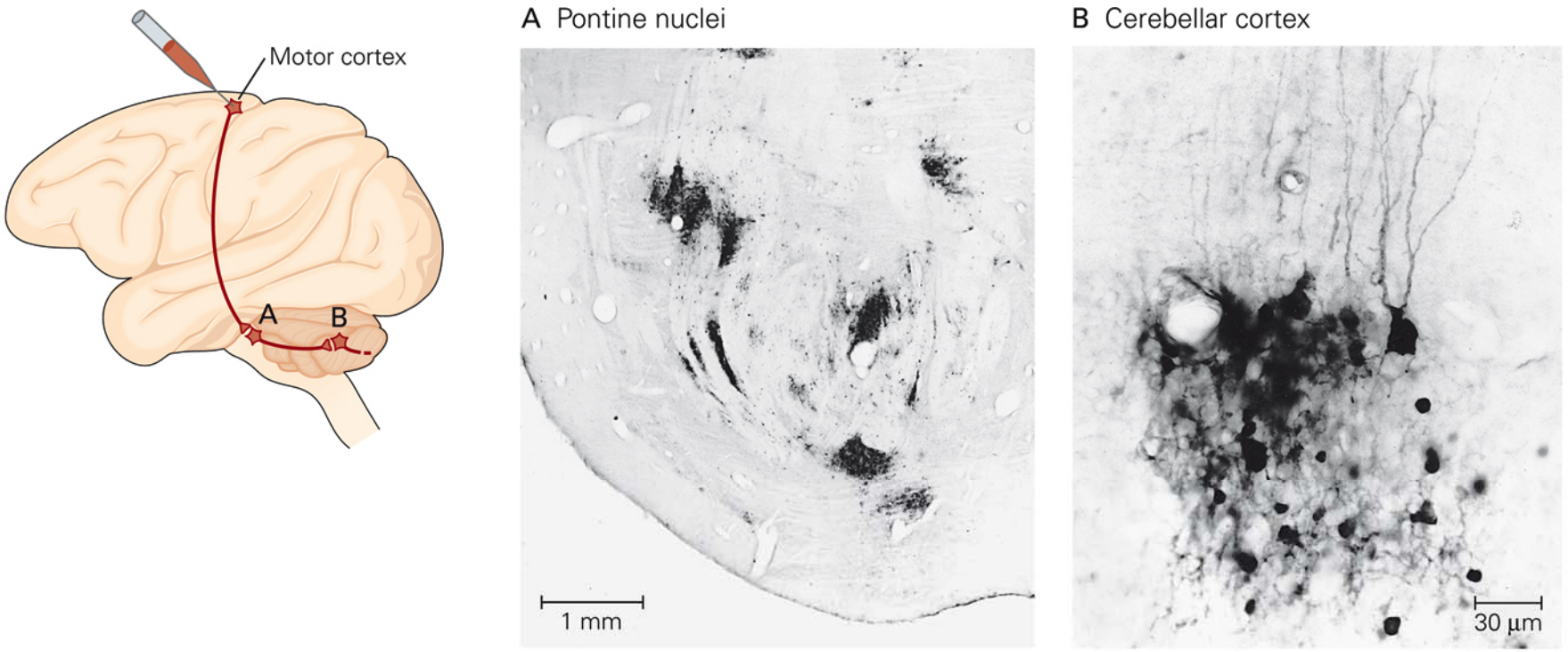

Figure 4–9 Axonal transport of the herpes simplex virus (HSV) is used to trace cortical pathways in monkeys. Depending on the strain, the virus moves in the anterograde or retrograde direction by axonal transport. In either direction it enters a neuron with which the infected cell makes synaptic contact. Here the projections of cells in the primary motor cortex to the cerebellum in monkeys were traced using an anterograde-moving strain (HSV-1 [H129]). Monkeys were injected in the region of the primary motor cortex that controls the arm. After 4 days the brain was sectioned and immunostained for viral antigen. Micrographs show the virus was transported from the primary motor cortex to second-order neurons in pontine nuclei (**A**) and then to third-order neurons in the cerebellar cortex (**B**). (Reproduced, with permission, from P. L. Strick.)

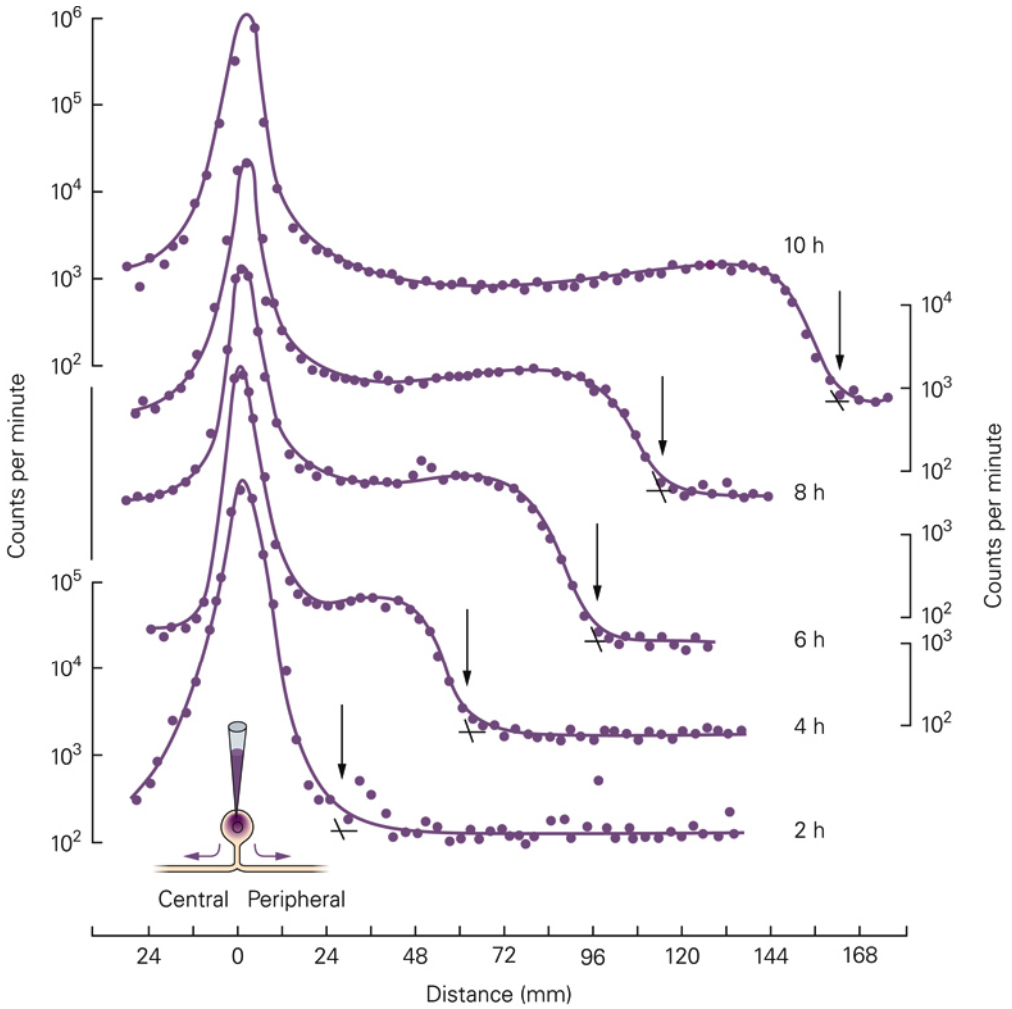

Figure 4–10 **Early experiments on anterograde axonal transport used radioactive labeling of proteins.** In the experiment illustrated here the distribution of radioactive proteins along the sciatic nerve of the cat was measured at various times after injection of [^{3}H]-leucine into dorsal root ganglia in the lumbar region of the spinal cord. To show transport curves from various times (2, 4, 6, 8, and 10 hours after the injection) in one figure, several ordinate scales (in logarithmic units) are used. Large amounts of labeled protein stay in the ganglion cell bodies but, with time, move out along axons in the sciatic nerve, so the advancing front of the labeled protein is progressively farther from the cell body (**black arrows**). The velocity of transport can be calculated from the distances of the front displayed at the various times. From experiments of this kind Sidney Ochs found that the rate of fast axonal transport is constant at 410 mm per day at body temperature. (Adapted, with permission, from Ochs 1972.)